NANO LETTERS

2007
Vol. 7, No. 9
2886−2891

A Biological Porin Engineered into a Molecular, Nanofluidic Diode

Henk Miedema,* Maarten Vrouenraets, Jenny Wierenga, Wim Meijberg, George Robillard, and Bob Eisenberg†

Biomade Technology Foundation, Nijenborgh 4, 9747 AG Groningen, The Netherlands, and Department of Molecular Biophysics and Physiology, Rush University Medical Center, 1750 West Harrison Street, Suite 1291, Chicago, Illinois 60612

Received July 11, 2007; Revised Manuscript Received July 31, 2007

ABSTRACT

We changed the nonrectifying biological porin OmpF into a nanofluidic diode. To that end, we engineered a pore that possesses two spatially separated selectivity filters of opposite charge where either cations or anions accumulate. The observed current inhibition under applied reverse bias voltage reflects, we believe, the creation of a zone depleted of charge carriers, in a sense very similar to what happens at the np junction of a semiconductor device.

In channels of large diameter (>100 nm), the interaction between the channel wall and electrolyte solution hardly affects the flow of ions. Under these conditions, geometric aspects and the bulk behavior of the electrolyte solution are determinant for ion flow dynamics. When we reduce the size and the channel diameter enters the nm range (<10 nm), this all changes dramatically. Then, the interaction between the solution and channel wall starts to dominate ionic flow. Given the charge density at the channel wall and the mobile ion species present, the extent of this interaction depends on the relative magnitudes of the channel diameter and the Debye screening length.[1−3] In general, the wider the channel, the lower the bulk concentrations needed to make this interaction become visible. Eisenberg[4−6] extensively explored and discussed the role of the potential profile (resulting from the distribution of both the permanent charge and mobile charges) on the flow of ions through nanopores. Manipulation of ion flow in structures of nanometer dimensions by means of surface charge and/or geometry has been proven successful, both in artificial[7−10] and proteinaceous nanochannels.[11−13] Rectification of ion flow requires an asymmetry in the geometry of the channel and/or the charge distribution along the channel wall.[14] Siwy and co-workers were able to produce rectification in a homogenously charged but geometrically asymmetric synthetic pore.[15] The alternative, a heterogeneously charged but geometrically symmetric pore, has proven more difficult, mainly because, until recently, the techniques for the chemical modification of nanochannels lacked the necessary spatial resolution. The recently developed technique of diffusion-limited patterning (DLP) is a first step to localized surface modification.[16] DLP was used already to synthesize a liquid-state diode out of a cylindrically shaped nanochannel with asymmetrical charge distribution[17] (see also Vlassiouk and Siwy,[18] but in a conically shaped pore).

From the perspective of nanochannel modification, biological ion channels are excellent starting points for nanofluidic devices. Compared to their solid-state counterparts and due to the tools of site-directed mutagenesis, protein channels allow modification at an unprecedented (sub)nanometer scale. With the 3D protein structure known, amino acid substitution at any given position is feasible (assuming the protein refolds properly and retains its functionality).

Ever since the elucidation of its 3D crystal structure,[19] the outer membrane protein F (OmpF) from *Escherichia coli* has been one of the most intensively studied ion channels. OmpF porin is a trimer protein composed of three identical and (more or less) independently operating monomers. Approximately halfway down the pore lumen, the diameter of each channel narrows down to about 1 nm. As shown by mutation studies, the following six amino acid residues, all located in the constriction zone, contribute significantly to the ion selectivity of OmpF (Table 1): K16, R42, R82, D113, E117, and R132.[13,20−26] The surface charge density in the constriction zone of OmpF is estimated to be as high as ∼300 mC/m^2 (e.g., for the presence of six positively charged arginines in a cylindrically shaped volume with a radius of 0.5 nm and a length of 1 nm; see the RR mutant in Table 1). This value is of the same order of magnitude as, for

* Corresponding author. E-mail: miedema@biomade.nl. Telephone: 31 50 3638070. Fax: 31 50 3634429.

† Department of Molecular Biophysics and Physiology, Rush University Medical Center.

10.1021/nl0716808 CCC: $37.00
Published on Web 08/11/2007

Table 1. Mutants Used in This Study[a]

Strain	Residues of 1st filter	Residues of 2nd filter
WT	K16 R42 R82 D113 E117 R132	E29 D37 D74 R167 R168
RR	K16 R42 R82 R113 R117 R132 (+4*e*)	E29 D37 D74 R167 R168
EE	K16 R42 R82 D113 E117 R132	E29 D37 D74 E167 E168 (-4*e*)
RREE	K16 R42 R82 R113 R117 R132 (+4*e*)	E29 D37 D74 E167 E168 (-4*e*)
RRR	K16 R42 R82 D113 E117 R132	R29 R37 R74 R167 R168 (+6*e*)

[a] Mutated residues are indicated in color. All net charges of the first and second selectivity filter (in between parenthesis) are based on the ionization state of the listed six (first) and five (second) residues of each filter and are given relative to the charge state of WT OmpF (see text).

Table 2. Rectification of WT and Mutant OmpF[a]

strain	salt	pH	I_{100}/I_{-100}
WT	0.1 NaCl	7.4	1.24 ± 0.03 (9)
WT	1 NaCl	7.4	0.99 ± 0.01 (9)
RR	0.1 NaCl	7.4	0.89 ± 0.03 (8)
EE	0.1 NaCl	7.4	0.81 ± 0.07 (5)
RREE	0.1 NaCl	7.4	0.22 ± 0.02 (5)
RREE	1 NaCl	7.4	0.65 ± 0.06 (6)
RREE	0.1 NaCl	3	0.46 ± 0.04 (3)
RRR	0.1 NaCl	7.4	3.14 ± 0.28 (5)

[a] The current rectification (I_{100}/I_{-100}) is defined as the ratio of absolute current magnitudes at 100 and −100 mV.

instance, the 60−100 mC/m^2 calculated by Stein et al.[10] for their synthetic nanochannels but much higher than the 1−5 mC/m^2 mentioned by Daiguji et al. .[27]

Depending on the ionic strength of the solution, the current−voltage relationship of WT OmpF shows either slight rectification (e.g., in 0.1 M NaCl) or nearly ohmic behavior (e.g., in 1 M NaCl), implying that the current magnitude at negative potential is the same as the one at positive potential (Table 2). Here we aimed to turn OmpF into a channel that shows strong current rectification. A recent study of Alacaraz et al.[28] demonstrated the rectifying properties of WT OmpF. However, to let WT OmpF behave as an ionic diode required the exposure of both ends of the channel molecule to solutions of different pH. In other words, (part of) the asymmetry needed to evoke rectification had to be attributed to the solutions used rather than to the protein itself. Our goal was to engineer an OmpF with intrinsic diode characteristics, i.e., one that rectifies even in symmetrical solutions. We reasoned that ion flow rectification requires the presence of two spatially separated areas where either cations or anions accumulate. The challenge thus is to design a pore that contains two oppositely charged selectivity filters. A molecular dynamics study of Im and Roux[29] motivated the selection of amino acid residues for a second selectivity filter. They calculated ion densities in slabs of 0.4 nm thickness and at different positions along the *z*-axis of OmpF. Their study revealed high densities of either cations or anions in the proximity of residues E29, D37, D74, R167, and R168, all located in the extracellular vestibule and on a distance of the constriction zone of, on average, 2.6 nm. Table 1 lists the mutants used in this study. The net charges of the two selectivity filters given in Table 1 are relative to those of WT OmpF and assume, at pH 7.4, either complete protonation (i.e., all lysines and arginines are assigned a charge of +1*e*) or complete ionization (i.e., all aspartates and glutamates are assigned a charge of −1*e*).[30,31]

Parts A−D of Figure 1 show side views of monomers of WT (A) and mutant OmpF (B−D). We should stress that the crystal structures of the OmpF mutants discussed here are still unknown. The images of these mutants as shown in Figure1B−D are derived from the crystal structure of WT OmpF (Figure 1A), with the orientation of the mutant residues optimized by SwissPdb Viewer software.

The electrophysiological characterization of (mutant) OmpF was performed using the planar lipid bilayer (PLB) technique (Figure 5A and see Miedema et al.).[25] In short, 3 M KCl/2% agar salt bridges connected the cis compartment to the headstage of the Axopatch 200B amplifier (Axon Instruments, Foster City, CA) and the trans compartment to ground. Neutral 1,2-diphytanoyl-*sn*-glycero-3-phosphocholine (DPhGPC, Avanti Polar Lipids) dissolved in decane (10 mg/mL) was used to paint a PLB across a 250 μm diameter aperture in a Delrin cuvette (Warner Inst., Hamden, CT). While stirring, ∼0.1−1 μL OmpF stock solution (containing 1% OPOE) was added to the trans side. Recording buffers contained NaCl or KCl and 20 mM HEPES (pK = 7.4) and were adjusted with *n*-methyl-D-glucamine (NMDG) to pH 7.4. The pH 3 solution contained 20 mM Na-acetate, 80 mM NaCl, and was adjusted to pH 3 with 1 N HCl. Data were low-pass filtered and digitized at 1 and 5 kHz, respectively. Current rectification is defined as the ratio of absolute current magnitudes at potentials of 100 and −100 mV (I_{100}/I_{-100}) with, importantly, all three OmpF monomers in the open state. The latter condition is essential to exclude rectification effects due to the opening and closing of individual OmpF monomers. As in solid state diodes, the degree of current rectification in nanofluidic channels is highly voltage dependent. To compare current magnitudes at potentials of ±100 mV was an entirely arbitrary choice.

The black trace in Figure 1E belongs to WT OmpF and shows the current response to a voltage ramp from −100 to 100 mV, in symmetrical 0.1 M NaCl, pH 7.4. The calculated I_{100}/I_{-100} of, on average, 1.24 (Table 2) indicates that the current−voltage relationship (*IV*) of WT demonstrates slight rectification (see also Nestorovich et al.[32] and Alcaraz et al.,[33] but note that the potential difference convention is opposite from the one used here). To determine the ion selectivity of the channel, we performed recordings under asymmetrical 1/0.1 M NaCl, pH 7.4 conditions (not shown). The slight

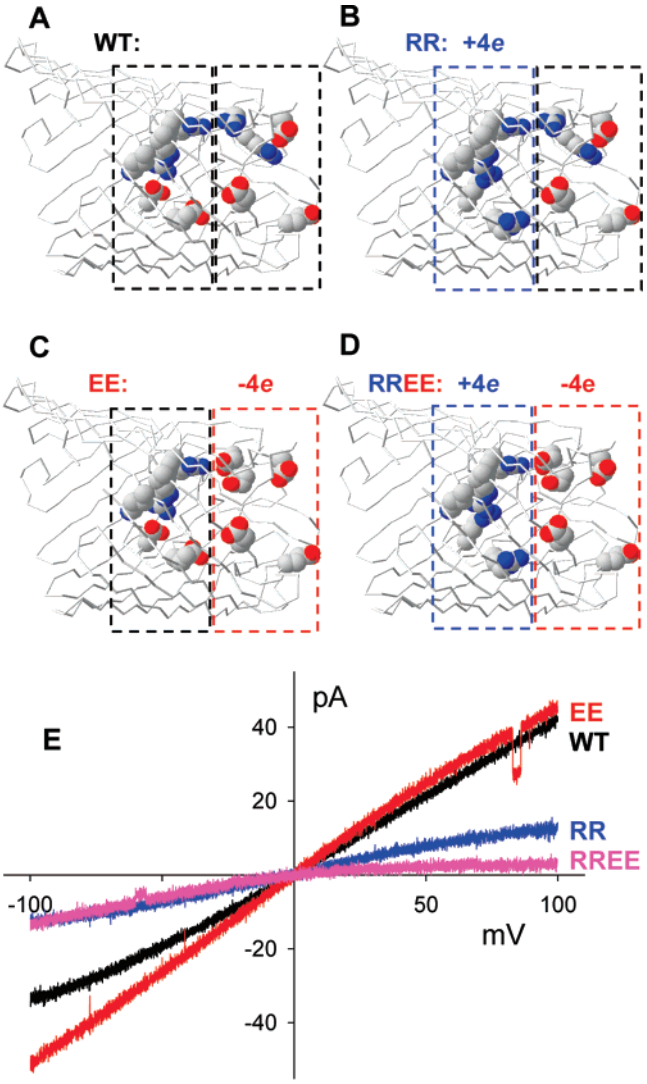

Figure 1. Side views of a single monomer of WT OmpF (A), the RR mutant (B), the EE mutant (C), and the RREE mutant (D). Images were produced by SwissPdb Viewer 3.7. Figure 1E shows the corresponding current profiles in response to a voltage ramp protocol from −100 to 100 mV (100 mV/s), recorded in symmetrical 0.1 M NaCl, pH 7.4 solutions. Note the temporal closing of a single monomer in the traces of the EE (at ∼80 mV) and RREE mutant (at ∼−60 mV).

cation selectivity of WT OmpF is evident from a measured reversal potential (E_{rev}) of −12.8 mV (Table 3).

The RR mutant (Figure 1B) has D113 and E117 in the constriction zone (hereafter referred to as the first selectivity filter) replaced with two arginines, whereas the second filter in the extracellular vestibule remained unchanged. Compared to WT, the current magnitudes are reduced, and with an I_{100}/I_{-100} of 0.89, the current rectification slightly inverted (blue trace in Figure 1E). As evident from measurements in 1/0.1 M NaCl solutions, adding a net charge of +4*e* to the first filter shifted E_{rev} more than 50 mV in the positive direction, implying the RR double mutant is, in contrast to WT protein, selective for anions.

In the EE mutant (Figure 1C), the first filter is WT-like but R167 and R168 of the second filter are substituted by two glutamates, resulting in a change of net charge of −4*e*.

Table 3. Selectivity and Conductance of WT and Mutant OmpF[a]

strain	E_{rev} in 1//0.1 M NaCl	g in 0.1 M NaCl
WT	−12.8 ± 1.7 (21)	413 ± 20 (20)
RR	38.3 ± 1.0 (5)	159 ± 10 (7)
EE	−27.5 ± 1.7 (7)	538 ± 18 (11)
RREE	28.7 ± 2.9 (15)	77 ± 7 (5)

[a] Reversal potentials (E_{rev}) were measured with 1 M NaCl, pH 7.4 in the cis compartment and 0.1 M NaCl, pH 7.4 in the trans compartment, resulting in an E_{Na} and E_{Cl} of −49 and 49 mV, respectively. Measured E_{rev} values have been corrected for a liquid junction potential of 11 mV. Conductance (g) in symmetrical 0.1 M NaCl, pH 7.4 is defined as the trimeric slope conductance at 0 mV, calculated in between −10 and 10 mV.

The currents through the pore of the EE mutant (red trace in Figure 1E) were similar in magnitude to those seen in WT. As was found for the RR mutant and compared to WT, the I_{100}/I_{-100} of 0.81 indicates a rectification of slightly reversed polarity. Note the jump in current level at ∼80 mV, representing the temporal closure of a single OmpF monomer. As reflected by the −15 mV shift of E_{rev}, the overall selectivity of the pore moved in the direction of improved cation selectivity. This change of E_{rev} clearly shows that residues outside the constriction zone can contribute to the ion selectivity of OmpF.

The measurements on the RR and EE mutant demonstrate that a change in either one of the filters affects the selectivity and conductance of the pore. However, the *IV* plots belonging to the two mutant proteins still lack signs of appreciable current rectification and in that sense still show WT-like behavior. We therefore designed a protein with mutations in both regions, the RREE mutant, with a change of net charge of +4*e* and −4*e* in its first and second selectivity filter, respectively (Figure 1D). The pink trace in Figure 1C shows that the presence of two oppositely charged selectivity filters significantly improves the rectification of the pore. With an I_{100}/I_{-100} of 0.22 and compared to the I_{100}/I_{-100} of 1.24 of WT, the rectification of this RREE mutant is enhanced by a factor >5. As for the overall ion selectivity, the E_{rev} of 28.7 mV is relatively close to that of the RR mutant (38.3 mV) and indicates that residues in the constriction zone still dominate the permeation properties of the pore even though residues located elsewhere can have an effect on the overall selectivity.

Figure 2 compares the rectification of a single trimer of the RREE mutant in response to a voltage ramp protocol (A) or a constant potential of ±100 mV (B), both in symmetrical 0.1 M NaCl, pH 7.4 solutions. Note that the two types of voltage protocols applied produce the same rectification. Current rectification can be caused by several mechanisms, among them (voltage-dependent) opening and closing (gating) of individual monomers. To distinguish and better visualize gating events, we performed recordings in 0.2 M KCl (Figure 2C) because OmpF conductance is higher in KCl than in NaCl. Although the degree of rectification in KCl is slightly less than in NaCl, the recordings in Figure 2 show a similar degree of rectification. As is obvious from the traces in, especially, KCl, the predominant and maximum

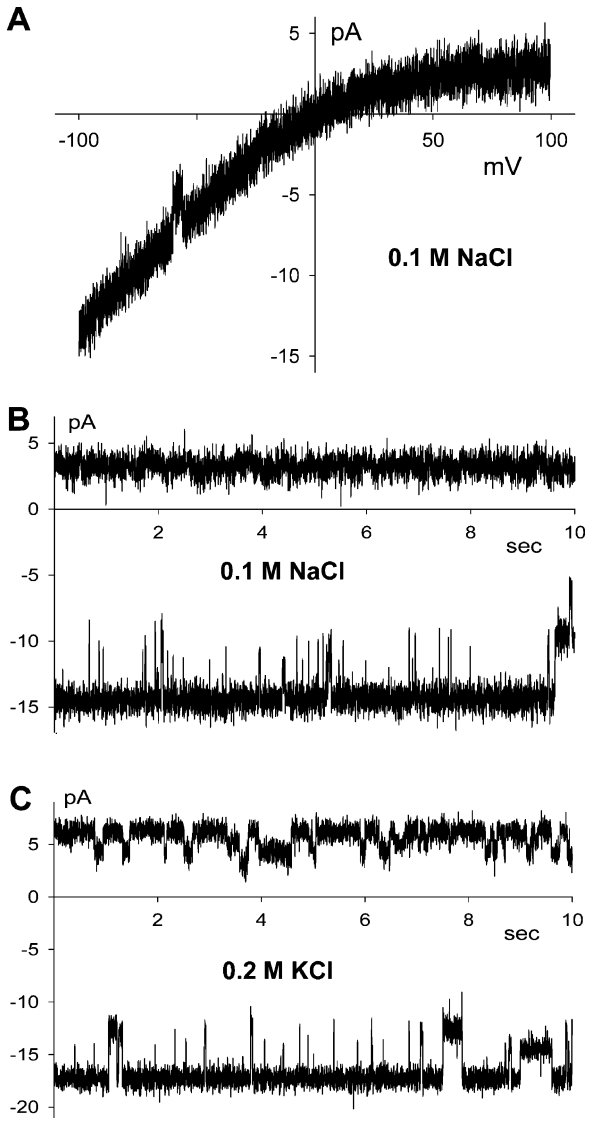

Figure 2. (A) The RREE trace of Figure 1E plotted at an enlarged scale. (B) Recordings on the RREE mutant at a constant potential of ±100 mV, in 0.1 M NaCl, pH 7.4. (C) Recordings on the RREE mutant at a constant potential of ±50 mV, in 0.2 M KCl, pH 7.4.

current levels clearly represent current magnitudes belonging to fully open trimer proteins. The relevance of this finding is that it disqualifies gating as the mechanism behind the current rectification. Instead, the (re)distribution of mobile ions inside the channel is at the heart of the phenomenon observed.

We also investigated the effect of ionic strength on the rectifying properties of the RREE mutant. Figure 3 A shows the *IV*'s of WT and the RREE mutant in symmetrical 1 M NaCl, pH 7.4 solutions. Under these high ionic strength conditions, the difference in current rectification between WT ($I_{100}/I_{-100} = 0.99$) and the RREE mutant ($I_{100}/I_{-100} = 0.65$) of 0.34 is only $^1/_3$ of the difference of 1.02 found in 0.1 M NaCl (Table 2). In addition, we tested the effect of low pH (in 0.1 M NaCl solutions). The pH 3 trace of Figure 3B shows an I_{100}/I_{-100} of 0.45, i.e., a value twice as large as the 0.22 observed at pH 7.4. Our interpretation is that low pH reduces the difference in net charge between the two filters because all five acidic residues (pK ∼ 4.4) of the second

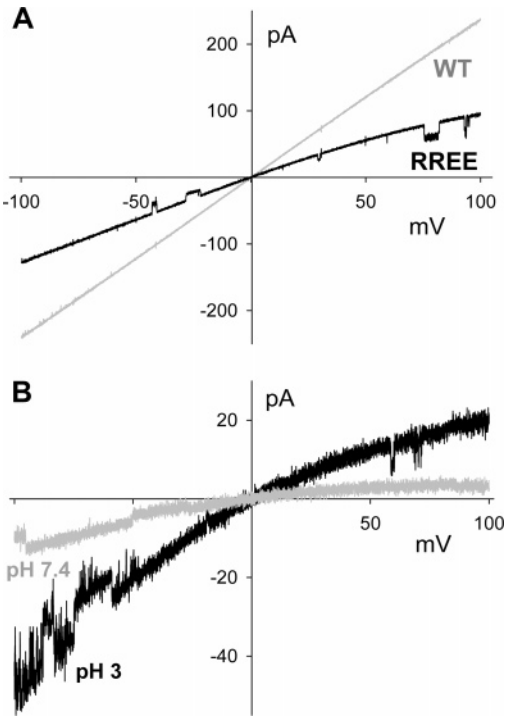

Figure 3. (A) Effect of 1 M NaCl (pH 7.4) on the current profiles of WT and the RREE mutant. (B) Effect of pH 3 on the current rectification of the RREE mutant, as recorded in 0.1 M NaCl solutions.

filter tend to become neutralized, whereas the net charge of the five arginines comprising the first filter remains unaffected. The effects of ionic strength and pH 3 on the rectifying properties of OmpF fit in the view that the mechanism of current rectification is electrostatic in nature.

If our interpretation is correct, we predict the rectification of the RREE mutant to invert upon switching both filters from position, i.e., make the first filter cation selective and the second filter anion selective. Even though the previously mentioned six amino acids in the constriction zone all contribute to the selectivity of OmpF, residue D113 dominates OmpF selectivity.[34] Cations strongly accumulate near D113 and mutation studies have shown that replacement of D113 by either a cysteine or a cysteine labeled with positively charged MTSET have a profound effect on the current profile and ion selectivity of OmpF.[13] We therefore started out with the RRR mutant (Table 1), i.e., with the first filter unchanged (and containing D113) but with E29, D37, and D74 all replaced with arginines, thereby changing the net charge of the second filter by 6*e* (Figure 4A). Compared to the rectification observed for the RREE mutant, the *IV* curve of the RRR mutant in Figure 4B shows an inversed current profile, reflected in an I_{100}/I_{-100} of 3.14. It is quite possible that the addition of more negative charge to the first filter further improves the current rectification of the RRR mutant. We attempted to introduce the RRR mutations as a second selectivity filter in the previously characterized LECE mutant (= K16L R42E R82C R132E).[13,25,26] Unfortunately, an extremely low refolding efficiency, due notably to the mutation at position 37, did not allow us to isolate a septuplet mutant protein that carries both the LECE

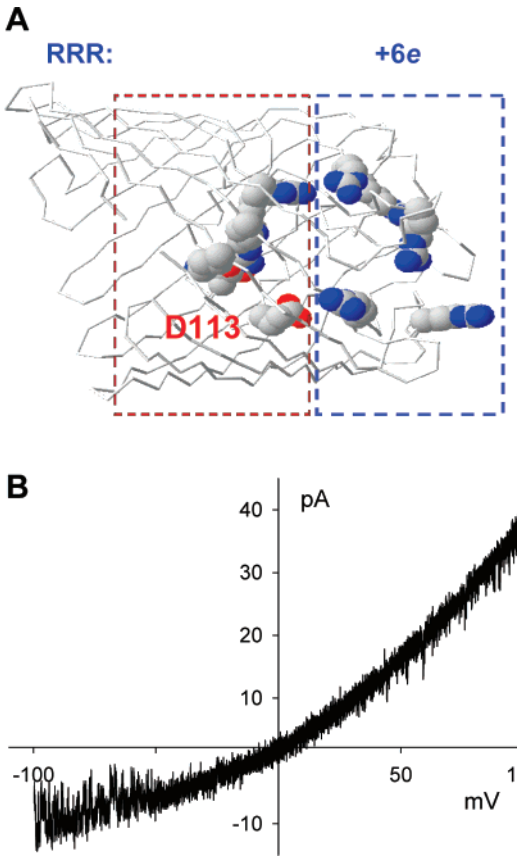

Figure 4. RRR mutant with in (A) a side view of a single monomer, with residue D113 indicated, and in (B) the current profile recorded in 0.1 M NaCl, pH 7.4.

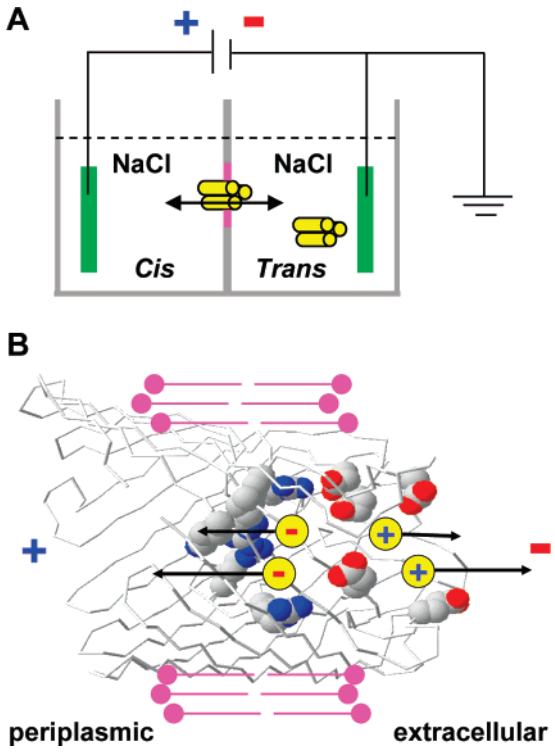

Figure 5. (A) Planar lipid bilayer set up with the cis and trans compartment connected by a trimeric OmpF porin (in yellow) reconstituted in the phospholipid lipid bilayer (in pink).The Ag/AgCl electrodes (in green) are indicated, the KCl salt bridges are not. After painting the bilayer and while stirring, OmpF protein was added to the (grounded) trans compartment. (B) Cartoon of a single monomer of the RREE mutant positioned in the phospholipid bilayer. The positively and negatively charged amino acid residues that make up the two selectivity filters are colored in blue and red, respectively, whereas the mobile ion species are colored yellow. Note that the orientation shown here, with the extracellular loops facing the trans compartment, corresponds to the current rectification seen in Figure 2. At positive potentials (i.e., cis positive), anions are attracted toward the periplasmic space and cations toward the extracellular solution in trans. The redistribution of ions causes the existence of a zone depleted of charge carriers, which in turn, causes less current to flow.

mutations in its first and the RRR mutations in its second filter. The refolding and ion selectivity of proteins that carry the D37R mutation is the focus of a forthcoming paper (Vrouenraets et al., in preparation).

Nonner et al.[35] already discussed the possibility that an area depleted of charge carriers (ions) may cause current rectification in ion channels. Eisenberg[4,5,36] pointed to the analogy between a solid-state and liquid-state or ionic diode. One similarity shows up in the expressions for the width of the depletion zone.[27] A difference between the two types of devices concerns the role the channel diameter plays in the liquid analogue. A prerequisite for a nanochannel to behave as an ionic diode is that the electrical double layers (EDL) do *not* overlap.[27] If the EDLs do overlap, the device becomes nonconductive independent of the voltage bias. Electroneutrality dictates that mobile ion species residing in the pore, on average, balance the permanent charge of the protein.[6] Given the small volume of (especially) the constriction zone and the permanent charge accumulated there, the local concentration of mobile ions can easily reach the molar range. The question to what extent the concept of EDL is still valid under those conditions remains rather speculative.

With the exception of the LECE-RRR mutant, the fact that the combination of all other mutations resulted in functional proteins that still insert into the membrane are able to transport ions across the bilayer, show ion selectivity, and gate prove that the mutant proteins retained their global structure. We fully realize, however, that our interpretation of (inversed) rectification in terms of the creation of a depletion zone hinges on the assumption that the orientation of the RREE and RRR mutants in the membrane is the same. The rationale behind this assumption is that we consider mutations in the pore lumen only and not at the external surface of the β-barrel. Indeed, when inserted into a PLB, the orientation of the majority of the individual OmpF porins ($\sim$95%) is the same.[32] The same is true for, for instance, maltoporin.[37] Apart from this consistency, the absolute orientation of reconstituted OmpF porin in the membrane is still open for discussion.[33] Given the relative position and net charges of the two selectivity filters, the current rectification of the RREE mutant should reveal the orientation of the protein (Figure 5). At positive potentials (i.e., cis positive), anions are attracted toward the periplasmic space and cations toward the extracellular solution in trans. The redistribution of ions causes the existence of a zone depleted of charge carriers which, in turn, causes less current to flow.

Following this reasoning, the current profile in Figure 2 implies that the OmpF protein enters the bilayer with the periplasmic surface first, whereas the extracellular loops remain at the side of protein addition (= trans). This finding is in accordance with earlier findings using a different approach.[38]

Finally, as already remarked, we still lack the crystal structure of the mutants described here. So the question to address is of how crucial detailed knowledge of the 3D structure actually is for understanding ion flow through a pore like OmpF. As discussed by Nonner and Eisenberg,[35] ion flow is relatively insensitive to atomic detail because Coulomb interactions are long-ranged and, despite local variations in charge distribution, the electropotential profile runs relatively smoothly (see also Boda et al.).[39] A recent study on several OmpF mutants of unknown crystal structure also emphasizes that the average electrostatic properties arising from the collective contribution of multiple residues rather than the precise 3D charge distribution are determinant for electrodiffusion through the pore.[40] It is for these reasons that we believe that the lack of the 3D structures of the RREE and RRR mutants does not invalidate our findings and interpretation given here.

In conclusion, nanotechnology can benefit enormously from our knowledge of the working mechanism of nanoscaled biological systems. To avoid reinventing the wheel, nanotechnology can mimic and design devices inspired by nature's nanomachines. In that tradition, we engineered a nonrectifying biological ion channel into a molecular diode. To do so, we extrapolated the mechanism responsible for the current rectification at an np junction of a semiconductor diode to the liquid state. Indeed, the underlying principle of the nanofluidic diode, we believe, is in respect to a depletion zone of charge carriers essentially the same as the one that causes a doped semiconductor to rectify. A challenging next step might involve the engineering of the ionic equivalent of an npn or pnp junction. This might be achieved by introducing a third selectivity filter located in the periplasmic vestibule of OmpF. However, as our attempts on the LECE-RRR mutant already show, the highest hurdle to take might be the refolding of a protein with that many mutations.

Acknowledgment. This research is supported by NanoNed, a nanotechnology program of the Dutch Ministry of Economic Affairs.

Supporting Information Available: Experimental details. This material is available free of charge via the Internet at http://pubs.acs.org.

References

(1) Daiguji, H.; Yang, P.; Majumdar, A. *Nano Lett.* **2004**, *4*, 137−142.
(2) Nishizawa, M.; Menon, V. P.; Martin, C. R. *Science* **1995**, *268*, 700−702.
(3) Wanunu, M.; Meller, A. *Nano Lett.* **2007**, *7*, 1580−1585.
(4) Eisenberg, B. *J. Membr. Biol.* **1996**, *150*, 1−25.
(5) Eisenberg, B. *J. Membr. Biol.* **1999**, *171*, 1−24.
(6) Eisenberg, B. *Biophys. Chem.* **2003**, *100*, 507−517.
(7) Karnik, R.; Fan, R.; Yue, M.; li, D.; Yang, P.; Majumdar, A. *Nano Lett.* **2005**, *5*, 943−948.
(8) Qiao, R.; Aluru, N. R. *Phys. Rev. Lett.* **2004**, *92*, 198301.
(9) Siwy, Z.; Heins, E.; Harrell, C. C.; Kohli, P.; Martin, C. R. *J. Am. Chem. Soc.* **2004**, *126*, 10850−10851.
(10) Stein, D.; Kruithof, M.; Dekker, C. *Phys. Rev. Lett.* **2004**, *93*, 035901.
(11) Gu, L.-Q.; Serra, M. D.; Vincent, J. B.; Vigh, G.; Cheley, S.; Braha, O.; Bayley, H. *Proc. Natl. Acad. Sci. U.S.A.* **2000**, *97*, 3959−3964.
(12) Lougheed, T.; Zhang, Z.; Woolley, G. A.; Borisenko, V. *Bioorg. Med. Chem.* **2004**, *12*, 1337−1342.
(13) Vrouenraets, M.; Wierenga, J.; Meijberg, W.; Miedema, H. *Biophys. J.* **2006**, *90*, 1202−1211.
(14) Gracheva, M. E.; Vidal, J.; Leburton, J.-P. *Nano Lett.* **2007**, *7*, 1717−1722.
(15) Siwy, Z. *Adv. Funct. Mater*. **2006**, *16*, 735−746.
(16) Karnik, R.; Castelino, K.; Duan, C.; Majumdar, A. *Nano Lett.* **2006**, *6*, 1735−1740.
(17) Karnik, R.; Duan, C.; Castelino, K.; Daiguji, H.; Majumdar, A. *Nano Lett.* **2007**, *7*, 547−551.
(18) Vlassiouk, I.; Siwy, Z. S. *Nano Lett.* **2007**, *7*, 552−556.
(19) Cowan, S. W.; Schirmer, T.; Rummel, G.; Steiert, M.; Ghosh, R.; Pauptit, R. A.; Jansonius, J. N.; Rosenbusch, J. P. *Nature* **1992**, *358*, 727−733.
(20) Lou, K.-L.; Saint, N.; Prilipov, A.; Rummel, G.; Benson, S. A.; Rosenbusch, J. P.; Schirmer, T. *J. Biol. Chem.* **1996**, *271*, 20669−20675.
(21) Saint, N.; Lou, K.-L.; Widmer, C.; Luckey, M.; Schirmer, T.; Rosenbusch, J. P. *J. Biol. Chem.* **1996**, *271*, 20676−20680.
(22) Schirmer, T. *J. Struct. Biol*. **1998**, *121*, 101−109.
(23) Schirmer, T.; Phale, P. S. *J. Mol. Biol*. **1999**, *294*, 1159−1167.
(24) Phale, P. S.; Philippsen, A.; Widmer, C.; Pahe, V. P.; Rosenbusch, J. P.; Schirmer, T. *Biochemistry* **2001**, *40*, 6319−6325.
(25) Miedema, H.; Meter-Arkema, A.; Wierenga, J.; Tang, J.; Eisenberg, B.; Nonner, W.; Hektor, H.; Gillespie, D.; Meijberg, W. *Biophys. J.* **2004**, *87*, 3137−3147.
(26) Miedema, H.; Vrouenraets, M.; Wierenga, J.; Eisenberg, B.; Gillespie, D.; Meijberg, W.; Nonner, W. *Biophys. J.* **2006**, *91*, 4392−4400.
(27) Daiguji, H.; Oka, Y.; Majumdar, A. *Nano Lett.* **2005**, *5*, 2274−2280.
(28) Alcaraz, A.; Ramírez, P.; Garćia-Giménez, E.; López, M. L.; Andrio, A.; Aguilella, V. M. *J. Phys. Chem. B* **2006**, *110*, 21205−21209.
(29) Im, W.; Roux, B. *J. Mol. Biol.* **2002**, *319*, 1177−1197.
(30) Karshikoff, A.; Spassov, V.; Cowan, S. W.; Ladenstein, R.; Schirmer, T. *J. Mol. Biol*. **1994**, *240*, 372−384.
(31) Varma, S.; Jakobsson, E. *Biophys. J.* **2004**, *86*, 690−704.
(32) Nestorovich, E. M.; Rostovtseva, T. K.; Bezrukov, S. M. *Biophys. J.* **2003**, *85*, 3718−3729.
(33) Alcaraz, A.; Nestorovich, E. M.; Aguilella-Arzo, M.; Aguilella, V. M.; Bezrukov, S. M. *Biophys. J.* **2004**, *87*, 943−957.
(34) Danelon, C.; Suenaga, A.; Winterhalter, M.; Yamato, I. *Biophys. Chem.* **2003**, *104*, 591−603.
(35) Nonner, W.; Chen, D. P.; Eisenberg, B. *Biophys. J.* **1998**, *74*, 2327−2334.
(36) Eisenberg, B. **2005**, q-bio.BM/0506016, http://arxiv.org.
(37) Danelon, C.; Brando, T.; Winterhalter, M. *J. Biol. Chem.* **2003**, *278*, 35542−35551.
(38) Bannwarth, M.; Schulz, G. E. *Protein Eng.* **2002**, *15*, 799−804.
(39) Boda, D.; Nonner, W.; Valisko, M.; Henderson, D.; Eisenberg, B.; Gillespie, D. *Biophys. J.* **2007**, 107.105478
(40) Aguilella-Arzo, M.; García-Celma, J. J.; Cervera, J.; Alcaraz, A.; Aguilella, V. M. *Bioelectrochem.* **2007**, *70*, 320−327.

NL0716808